doi: 10.1038/nature06290

Molecular basis of RNA-dependent RNA polymerase II activity

Elisabeth Lehmann, Florian Brueckner, and Patrick Cramer

Gene Center Munich and Center for integrated Protein Science CiPS^{M}, Department of Chemistry and Biochemistry, Ludwig-Maximilians-Universität München, Feodor-Lynen-Strasse 25, 81377 Munich, Germany.

Supplemental Materials

Supplementary Table 1

Mass spectrometric analysis of RNA species observed after incubation of scaffold RdRP with Pol II and NTPs (compare Fig. 2a).

RNA product	Incorporated nucleotides	Theoretical mass[1]	Observed mass
Reactant RNA	-	5664	5663, 5665
+1	G	6009	6009, 6010
+2	GU	6315	6317[2]
+3	GUC	6620	6619[2], 6621[2]
+4	GUCA	6949	6949, 6951
+5	GUCAA	7279	7279
+6	GUCAAG	7624	7624
+7	GUCAAGC	7929	7929
+8	GUCAAGCU	8235	8235, 8236
Template strand	-	8342	8342

[1]Calculated with Mongo Oligo Mass Calculator and using a molecular weight for 6-FAM of 537.5 Dalton.

[2]Observed after incubations with NTP subsets.

Supplementary Table 2

Crystallographic data and refinement statistics for the Pol II complexes with the artificial scaffold RdRP-ss6 (Figs. 2, S3 and the HDV-derived 6 bp stem-loop (Fig. 4a).

Pol II complex	RdRP	HDV
Data collection[1]		
Space group	$C222_1$	$C222_1$
Cell dimensions		
a, *b*, *c* (Å)	222.7, 393.8, 283.5	223.3, 394.9, 284.1
Wavelength (Å)	1.0716	0.9999
Resolution (Å)	50.0-3.8 (3.94-3.8)[2]	50.0-4.0 (4.14-4.0)[2]
R_{sym}	0.077 (0.335)	0.149 (0.479)
$I/\sigma I$	21.4 (6.8)	12.4 (4.2)
Completeness (%)	99.9 (100.0)	100.0 (99.9)
Redundancy	8.5 (8.5)	8.5 (7.7)
Refinement[3]		
Resolution (Å)	50.0-3.8	50.0-4.0
No. reflections	121,604	104,655
R_{work}/ R_{free}[4]	0.212/0.246	0.216/0.241
No. atoms		
Protein	31,207	31,207
Nucleic acid	400	292
Ligand/ion	9	9
B-factors		
Protein	127.4	126.1
Nucleic acid	195.3	166.4
Ligand/ion	111.9	106.7
R.m.s deviations		
Bond lengths (Å)	0.008	0.008
Bond angles (°)	1.47	1.49

[1]Diffraction data were collected in 0.25° increments at beamline X06SA of the Swiss Light Source and were processed with program XDS[1] (RdRP-ss6) or DENZO[2] (HDV stem-loop).

[2]Highest resolution shell is shown in parenthesis.

[3]Structures were solved by molecular replacement with the program Phaser[3], using the complete 12-subunit Pol II[4] as search model. The nucleic acids were built stepwise into unbiased F_o-F_c electron density maps (Fig. 2a). Model building was done with program O[5], and refinement with CNS[6].

[4]For free R-factor calculation, we excluded from refinement the same set of reflections that had been excluded from previous Pol II structure determinations[7,8].

Supplementary Figure 1: Comparison of misincorporation events during RNA elongation with scaffolds RdRP and the corresponding scaffold DdRP that comprises a DNA template strand.

a, Scaffolds RdRP and DdRP are depicted. The RNA product strands are in raspberry (RdRP) or red (DdRP), the RNA template strand is in orange and the DNA template in blue. The FAM fluorescent label is shown as a green diamond. The same color code is used throughout.

b, RNA synthesis with scaffold RdRP (lane 1-10) and DdRP (lane 11-20). Lane 1 and 11 show the fluorescently labeled reactant RNA. In lanes 2-10 and 11-20, scaffold were incubated with pure Pol II (Methods) and then incubated for 5 min with different types and subsets of NTPs as indicated. Despite the faster rate of synthesis with scaffold DdRP, the pattern of misincorporations is highly similar.

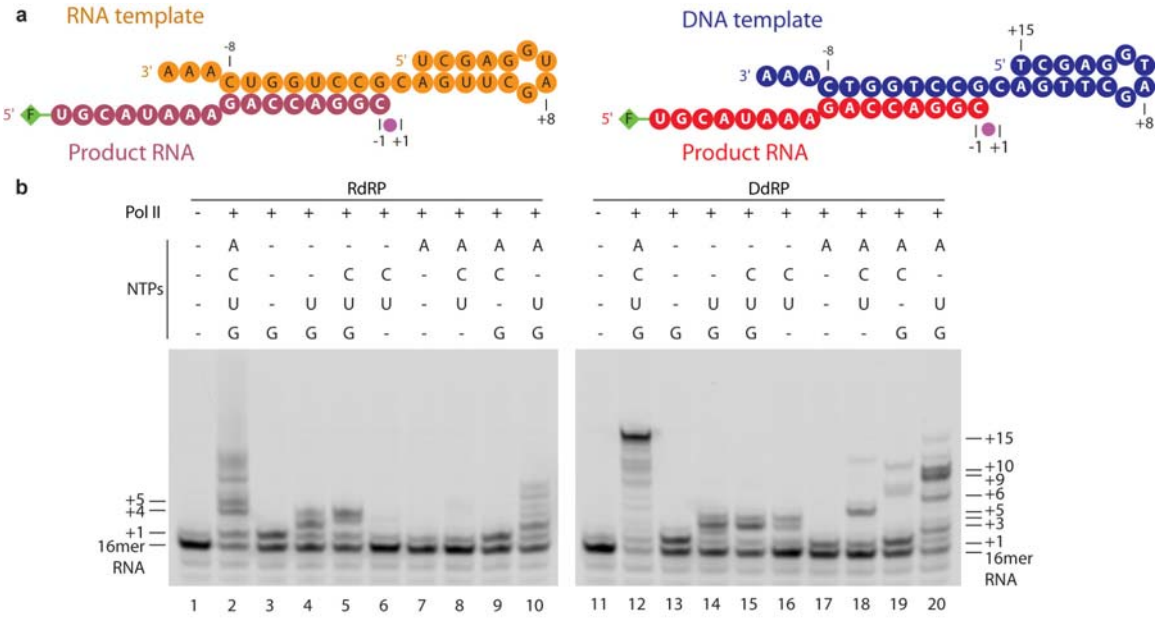

Supplementary Figure 2: Pol II RdRP activity on alternative artificial scaffolds.

a, Alternative RdRP scaffolds. Nucleotides that are incorporated by Pol II RdRP activity are shown as raspberry open circles. The stalling position is indicated.

b-d, RNA synthesis with alternative RdRP scaffolds shown in **a**. Lane 1 always shows the fluorescently labeled reactant RNA. In lanes 2-6, alternative RNA scaffolds were incubated with pure Pol II and NTPs (compare Methods).

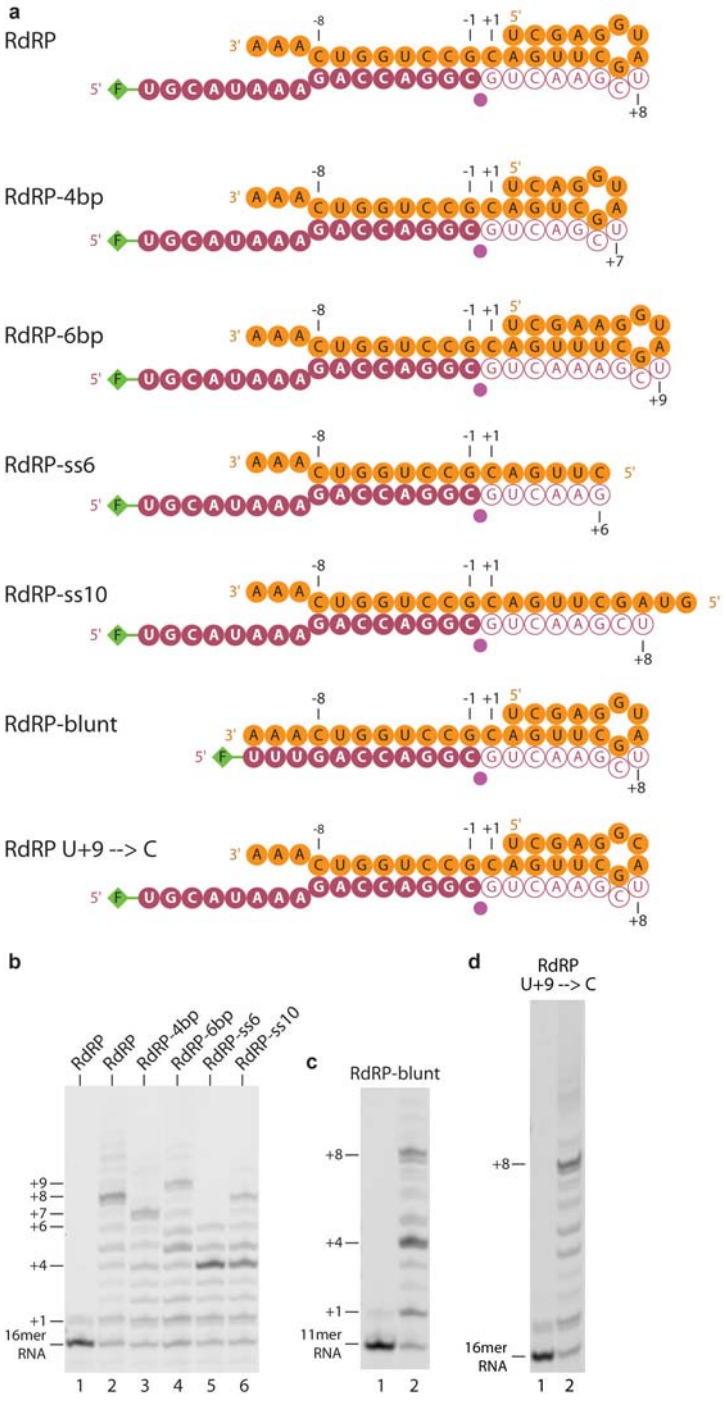

Supplementary Figure 3: Additional electron density maps for the RNA template-product duplex in the Pol II RdRP EC.

a, Difference Fourier omit map obtained using phases from the final model with nucleic acids removed. The view is as in Fig. 2. The RNAs are shown as stick model with the RNA product and template in raspberry and orange, respectively. The F_o-F_c map at 2.2σ is shown as green mesh.

b, The final observed $2F_o$-F_c electron density map calculated with model phases is shown in blue with the contour level as indicated. Views are related by a 90° rotation around a horizontal axis. Figures were prepared with PyMOL (DeLano Scientific).

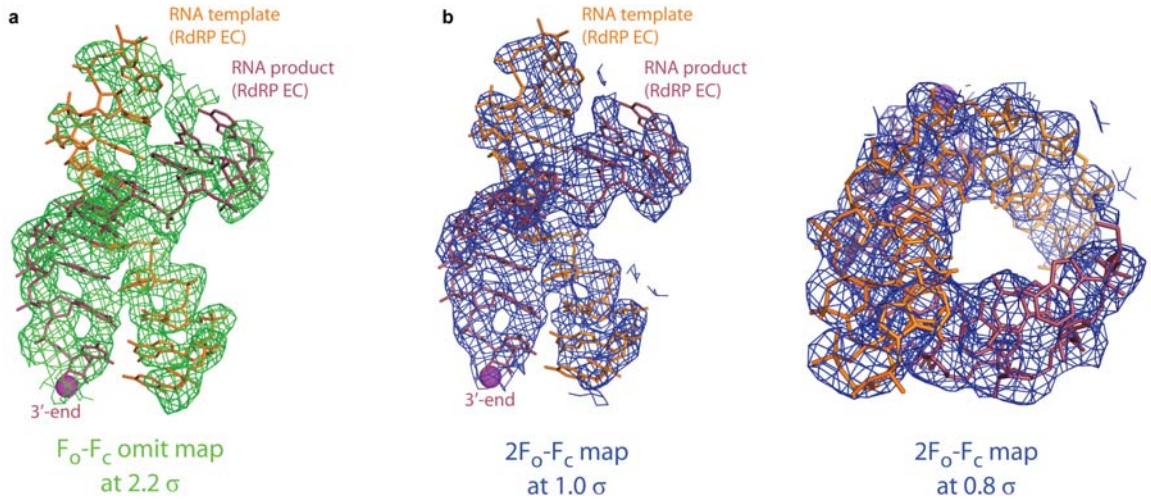

Supplementary Figure 4: Scaffolds RdRP and DdRP compete for Pol II in RNA elongation assays.

a, Nucleic acid scaffolds used for competition analysis.

b, Competition assays. Pol II and scaffold 1 were assembled as described (Methods). Scaffold 2 was added in relative amounts (1, 2, or 5-fold molar excess) with respect to scaffold 1 as indicated, and incubated for 10 min at 20 °C. DdRP and RdRP scaffolds used as scaffolds 2 were identical to scaffolds 1 except that an 11mer product RNA was used, which lacked the five 5' residues and the fluorescent label ("cold" competitors). In control experiments (lanes 1 and 5) transcription buffer was added instead. The mixture was incubated with 1 mM NTPs for 5 min at 28 °C. Without competing scaffold 2 the final product of each reaction is observed (+8 in lane 1, +15 in lane 5), respectively. With increasing amounts of scaffold 2 (lanes 2-4 and 5-8), the final product of the reaction disappears and the reactant RNA remains, indicating competition for Pol II. Competition is observed independent of the order of scaffold addition.

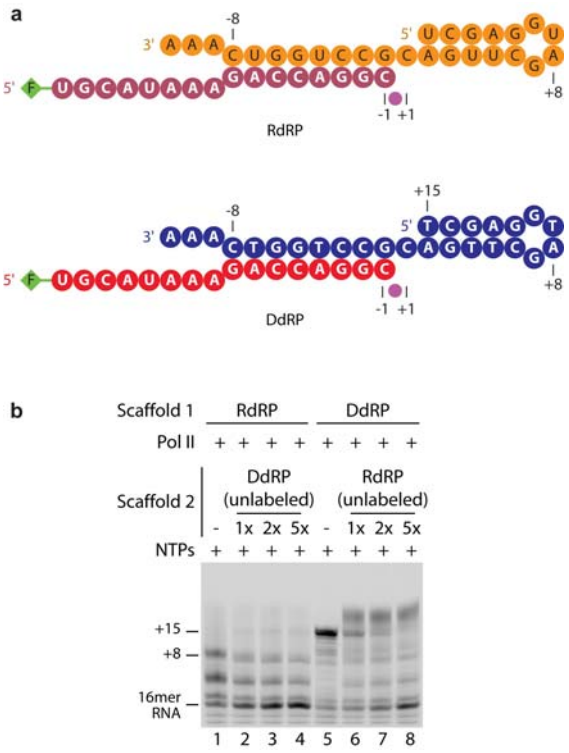

Supplementary Figure 5: Mutational analysis of the loop in the HDV-derived scaffold. **a,** RNA scaffolds HDV and HDV-AG, which contains a CU->AG sequence alteration in the terminal loop.

b, Comparison of RNA extension products obtained with RNA scaffolds shown in **a**. Lanes 1 and 3 show the fluorescently labeled reactant RNAs. Lanes 2 and 4 show extension products. There are no significant differences in the pattern of extension products.

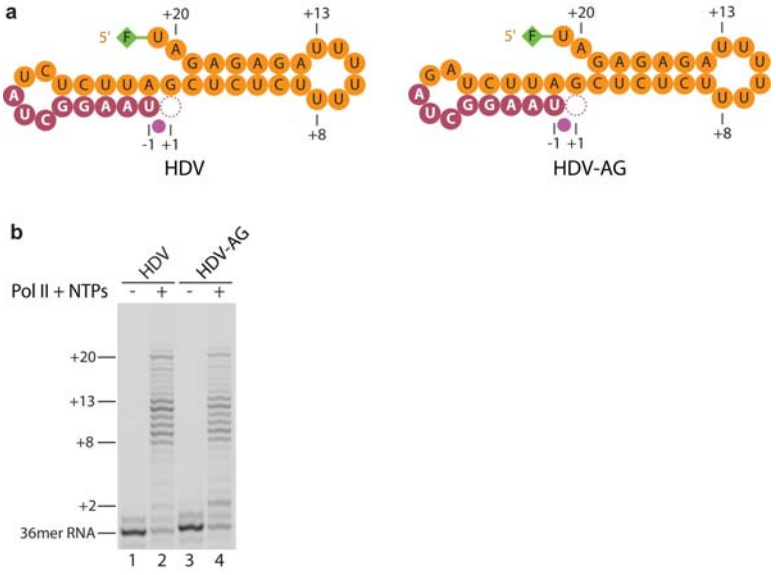

Supplementary Figure 6: Templated RNA elongation of an 11 bp stem-loop derived from pCPG79 RNA used in previous studies[9].

a, Mfold secondary structure prediction of pCPG79 RNA. Cleavage sites observed previously by TFIIS-induced cleavage[9] are indicated.

b, RNA scaffold derived from the predicted pCPG79 RNA structure in **a**. The scaffold corresponds to the product obtained after the previously observed RNA cleavage at the central cleavage site[9]. The scaffold consists of the 3' stem-loop of pCPG79 RNA with an 11 bp stem and a two-nucleotide 5'-overhang.

c, RNA elongation assay with the scaffold shown in **b**. Lane 1 shows the fluorescently labeled reactant RNA. Reactions were incubated with different NTPs or subsets of NTPs for the time indicated (lanes 2-10). Only CTP leads to addition, indicating GMP-templated RdRP activity.

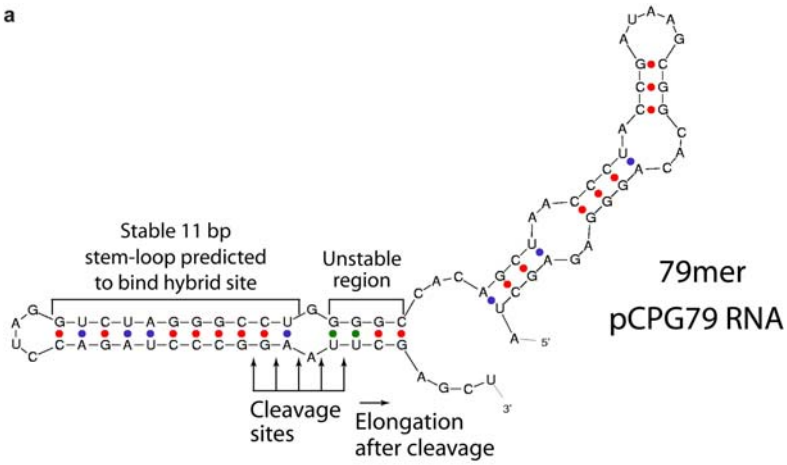

References

1. Kabsch, W. *J. Appl. Cryst.* **26**, 795-800 (1993).
2. Otwinowski, Z. & Minor, W. Processing of X-ray diffraction data collected in oscillation mode. *Meth. Enzym.* **276**, 307-326 (1996).
3. McCoy, A. J., Grosse-Kunstleve, R. W., Storoni, L. C. & Read, R. J. Likelihood-enhanced fast translation functions. *Acta Crystallogr D Biol Crystallogr* **61**, 458-64 (2005).
4. Armache, K.-J., Mitterweger, S., Meinhart, A. & Cramer, P. Structures of complete RNA polymerase II and its subcomplex Rpb4/7. *J. Biol. Chem.* **280**, 7131-7134 (2005).
5. Jones, T. A., Zou, J. Y., Cowan, S. W. & Kjeldgaard, M. Improved methods for building protein models in electron density maps and the location of errors in these models. *Acta Cryst.* **A47**, 110-119 (1991).
6. Brunger, A. T. et al. Crystallography & NMR system: A new software suite for macromolecular structure determination. *Acta Crystallogr D Biol Crystallogr* **54**, 905-21 (1998).
7. Brueckner, F., Hennecke, U., Carell, T. & Cramer, P. CPD damage recognition by transcribing RNA polymerase II. *Science* **315**, 859-62 (2007).
8. Kettenberger, H., Armache, K.-J. & Cramer, P. Complete RNA polymerase II elongation complex structure and its interactions with NTP and TFIIS. *Mol. Cell* **16**, 955-965 (2004).
9. Johnson, T. L. & Chamberlin, M. J. Complexes of yeast RNA polymerase II and RNA are substrates for TFIIS-induced RNA cleavage. *Cell* **77**, 217-224 (1994).